

Article

Collapse of Silicon Valley Bank and USDC Depegging: A Machine Learning Experiment

Papa Ousseynou Diop, Julien Chevallier *  and Bilel Sanhaji 

Economics Department, Université Paris 8 (LED), 2 Rue de la Liberté, 93526 Saint-Denis, France; papa-ousseynou.diop@anciens.univ-paris1.fr (P.O.D.); bilel.sanhaji@univ-paris8.fr (B.S.)

* Correspondence: julien.chevallier04@univ-paris8.fr

Abstract: The collapse of Silicon Valley Bank (SVB) on 11 March 2023, and the subsequent depegging of the USDC stablecoin highlighted vulnerabilities in the interconnected financial ecosystem. While prior research has explored the systemic risks of stablecoins and their reliance on traditional banking, there has been limited focus on how banking sector shocks affect digital asset markets. This study addresses this gap by analyzing the impact of SVB's collapse on the stability of major stablecoins—USDC, DAI, FRAX, and USDD—and their relationships with Bitcoin and Tether. Using daily data from October 2022 to November 2023, we found that the SVB incident triggered a series of depegging events, with varying effects across stablecoins. Our results indicate that USDC, often viewed as one of the safer stablecoins, was particularly vulnerable due to its reliance on SVB reserves. Other stablecoins experienced different impacts based on their collateral structures. These findings challenge the notion of stablecoins as inherently safe assets and underscore the need for improved risk management and regulatory oversight. Additionally, this study illustrates how machine learning models, including gradient boosting and random forests, can enhance our understanding of financial contagion and market stability.

Keywords: stablecoin; depeg; USDC; Silicon Valley Bank; bank run; machine learning

JEL Classification: E44; G15; Q02



Citation: Diop, P.O.; Chevallier, J.; Sanhaji, B. Collapse of Silicon Valley Bank and USDC Depegging: A Machine Learning Experiment. *FinTech* **2024**, *3*, 569–590. <https://doi.org/10.3390/fintech3040030>

Academic Editor: David Roubaud

Received: 4 October 2024

Revised: 28 November 2024

Accepted: 11 December 2024

Published: 13 December 2024



Copyright: © 2024 by the authors. Licensee MDPI, Basel, Switzerland. This article is an open access article distributed under the terms and conditions of the Creative Commons Attribution (CC BY) license (<https://creativecommons.org/licenses/by/4.0/>).

1. Introduction

On 11 March 2023, the collapse of Silicon Valley Bank (SVB) highlighted the critical dependence of stablecoins, such as USD Coin (USDC), on traditional banking systems for their reserves, thus intensifying systemic risks within the financial landscape. Concerns about fractional reserves prompted investors to divest from USDC, resulting in a depegging of the currency until the Federal Deposit Insurance Corporation (FDIC) provided assurances for SVB deposits. To maintain stability and foster investor confidence, it is imperative that stablecoins prioritize the acquisition of liquid, low-risk assets, such as short-term US Treasury securities. During the depeg, investors demonstrated a preference for transferring their holdings from USDC to Tether (USDT) or fiat currency. SVB's downfall stemmed from its significant exposure to long-term bonds in a rising interest rate environment, which revealed inherent vulnerabilities in its reserve allocation strategies. In contrast to the algorithmic failure of Terra-LUNA or the scrutiny faced by USDT, USDC's crisis was primarily driven by its partial reserve exposure to SVB. Additionally, Circle's reliance on the FDIC bailout has highlighted the need for stablecoins to adopt robust and transparent crisis management frameworks. This approach is essential for enhancing resilience and mitigating potential risks in the future.

On 9 March 2023, the California Department of Financial Protection and Innovation closed Silicon Valley Bank due to a bank run triggered by concerns over its financial stability. As pictured in Figure 1, this marked the second-largest bank failure in the USA

since the collapse of Washington Mutual in 2008 [1]. The announcement caused panic among investors, leading to a rush to swap their USDC tokens for more resilient options like BTC and ETH. On 11 March 2023, this situation resulted in the depegging of USDC, DAI, and FRAX [2], as illustrated by the price level-volume analysis of seven cryptocurrency pairs in Figure 2. As shown in Table 1, a careful examination yielded the detection of volume spikes for four stablecoins, particularly around the date of the SVB collapse: USDC, USDD, FRAX, and DAI. The goal is to detect whether the maximum volume recorded that day is significantly higher than the surrounding data, typically recorded as a spike in trading when it exceeds twice the average volume. This situation resembled the significant stablecoin run that occurred when Terra, the fourth-largest stablecoin at the time, faced a run and eventual collapse in early May 2022 [3]. In both instances, there was a trend of investors seeking safer options, leading to negative repercussions for other algorithmic stablecoins and those backed by riskier assets, while stablecoins backed by relatively safer assets experienced increased demand.



Figure 1. Triggering event: the SIVBQ collapsed in March 2023. Note: *SIVBQ* is the ticker of the stock price for the SIVB Financial Group in USD. Source: Yahoo Finance.

Table 1. Detected volume spikes for cryptocurrencies around the SVB crash on 11 March 2023.

Cryptocurrency	Date of Spike	Volume
USDC	11 March 2023	26,682,206,827
USDD	11 March 2023	115,850,558
FRAX	11 March 2023	399,581,581
DAI	11 March 2023	4,642,451,631

Note: *USDC* is Circle’s USD Coin, *USDD* is Tron’s USDD, *FRAX* represents Frax Finance’s stablecoin, and *DAI* is MakerDAO’s DAI. All cryptocurrency pairs are quoted against the USD.

The insolvency of Silicon Valley Bank in March 2023 resulted in a significant event within the cryptocurrency sphere: the temporary depegging of USD Coin (USDC) [1]. USDC, a stablecoin designed to maintain a consistent value pegged to the US dollar, encountered exceptional volatility following the failure of SIVB, a crucial banking partner for Circle, the issuer of USDC [4]. This event not only disrupted the stability of USDC but also underscored the vulnerabilities and interdependencies between stablecoins and traditional financial institutions [3]. Gaining an understanding of the causes and repercussions of the USDC depeg offers crucial insights into the stability and resilience of digital assets and their interactions with traditional banking sector crises [2]. Additionally, it has been reported that, in China, there exists a positive correlation between bank profitability and the advancement of fintechs [5].

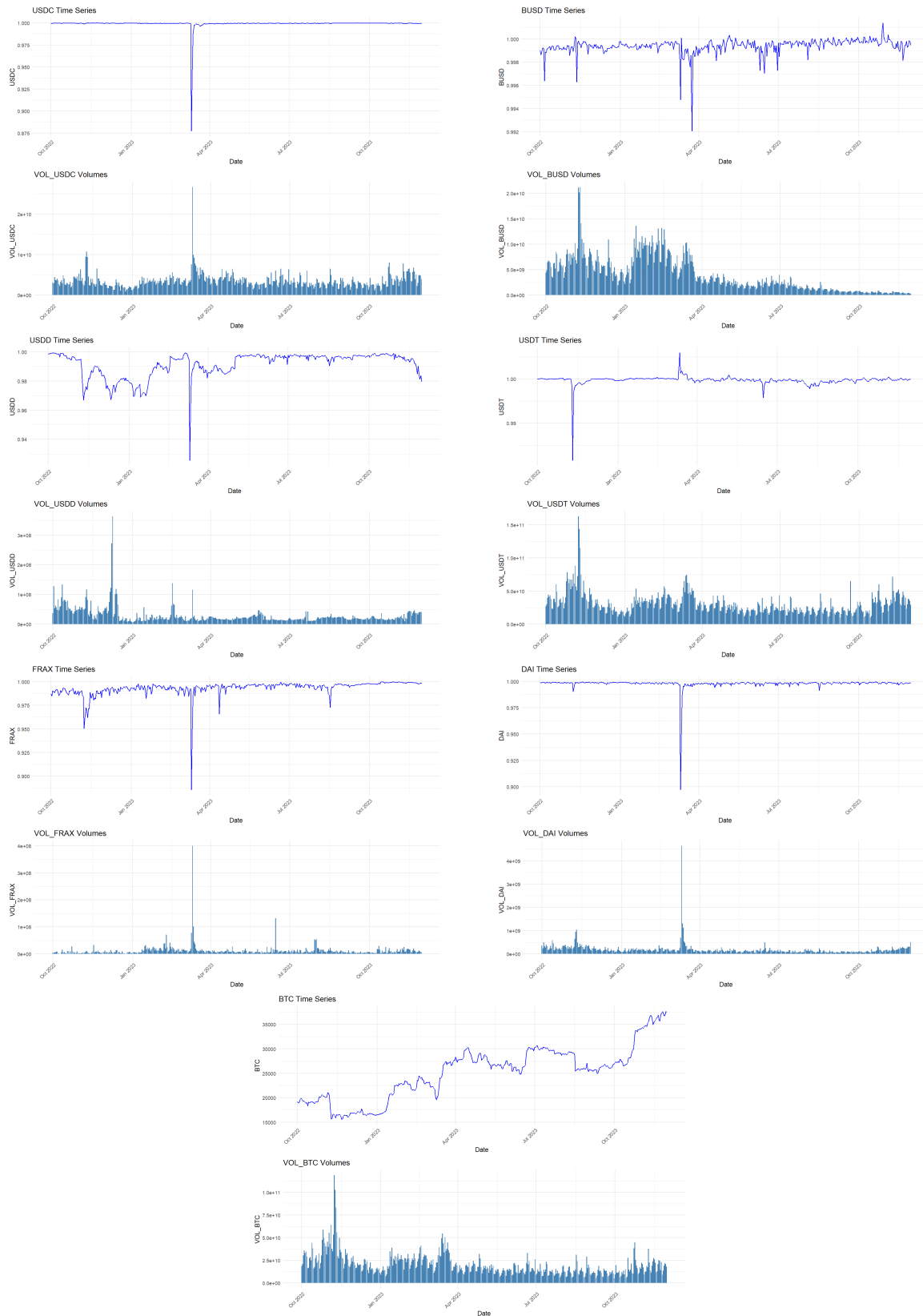


Figure 2. Time Series and Volumes for 7 cryptocurrency pairs. Note: From top to bottom and left to right, *USDC* is Circle’s stablecoin in USD, *BUSD* is Binance’s stablecoin in USD, *USDD* is Tron’s stablecoin in USD, *USDT* is Tether’s stablecoin in USD, *FRAX* is Frax Finance’s stablecoin USD in USD, *DAI* is MakerDAO Foundation’s DAI in, and *BTC* is the Bitcoin price in USD. For each cryptocurrency, *VOL* indicates the volumes traded. Source: Yahoo Finance.

Stablecoins experienced increased instability following the collapse of Silicon Valley Bank in March 2023 [6]. Similarly to the events of May 2022, cryptocurrency investors promptly responded to the news by divesting or redeeming their USDC tokens [7]. In contrast to the May 2022 incident, which involved riskier stablecoins, the turbulence in March 2023 predominantly impacted USDC, previously considered one of the safest stablecoins due to its backing by Treasury securities and bank deposits [8]. This instability also affected DAI and FRAX, both of which relied partly on USDC as collateral [9]. It is thus logical that investors transitioned from USDC to other stablecoins perceived as more secure at the time, particularly those backed by traditional assets, notably Tether (USDT). For a pioneering analysis of the inter-relationships between Tether and Bitcoin, interested readers are referred to [10].

Stablecoins have gained significant traction in response to the price volatility of leading cryptocurrencies like BTC and ETH [11], which undermines their capacity to function as stable stores of value [12]. Stablecoins are digital assets engineered to maintain a consistent value, often pegged at USD 1 [13], through various mechanisms such as asset reserves or sophisticated algorithms [14]. The stablecoin market is anticipated to experience substantial growth in trading volumes and attract heightened interest from market practitioners [15]. The market capitalization of stablecoins has witnessed a remarkable surge, escalating from USD 5 billion in 2019 to approximately USD 180 billion in 2022 before moderating to nearly USD 120 billion by 2023 [7]. There are four primary categories of stablecoins: algorithmic stablecoins (FRAX, USTC, USDD), stablecoins backed by traditional financial assets (USDC, USDT), stablecoins backed by crypto assets such as Bitcoin and Ethereum (DAI, LUSD), and commodity-backed stablecoins (PAXG, SLVT) [8]. In just a decade since the introduction of the first stablecoin, the count of “active” stablecoins—defined as those with a positive market capitalization—has surged to over 60. Notably, Tether (USDT) and USD Coin (USDC) stand out as the most prominent among them thus far [16]. USD Coin is an asset-backed stablecoin designed to maintain a steady value of USD 1, and is fully supported by reserves comprising cash and short-term treasuries. Investors favor stablecoins as a hedge against the unpredictable fluctuations of the cryptocurrency market and for their potential to generate passive earnings through staking or lending mechanisms [7]. Additionally, stablecoins can offer funding opportunities to facilitate business credit flows [17].

Regrettably, stablecoins are encountering depegging challenges, resulting in unprecedented losses within the DeFi ecosystem [18]. Following the Luna crash, it has become evident once again that stablecoins are not as resilient as previously assumed, exemplified by the depegging of USDC. On Friday, 9 March 2023, Circle disclosed that USD 3.3 billion of its approximately USD 40 billion reserve was deposited with Silicon Valley Bank (SIVB), marking one of the most significant bank collapses in recent US history since Washington Mutual in 2008 [12]. By the conclusion of 2022, SIVB had amassed a total of USD 110.4 billion in assets and collected deposits amounting to USD 88.6 billion. It is noteworthy that cryptocurrency businesses accounted for 30% of their deposits as early as 2021 [4].

The term “stablecoins” has generated discussion regarding its appropriateness [19]. Are recent events indicative of a temporary setback, or do they reveal a fundamental flaw in the cryptocurrency market? This study underscores the risks associated with cryptocurrency trading and emphasizes the vital relationship between traditional finance and DeFi. It leverages a machine learning model, building upon insights from [20], to enhance forecasting dynamics. This study expands linear and model selection tests to a multi-equation framework, exploring neural networks, regression trees, boosting, gradient boosting, and random forests. It considers stablecoins as outputs and utilizes SIVB stock as inputs, utilizing daily data from October 2022 to November 2023. Our findings significantly contribute to the existing literature, particularly in studies that delve into the interdependence between cryptocurrencies and stablecoins, as well as the crucial connections between the DeFi sector and the banking system.

In our assessment of SIVB’s default, the following findings were observed: (i) the gradient boosting machine demonstrated superior performance compared to the linear

benchmark, followed by stacked random forests. (ii) Particularly noteworthy is the high impact on the stablecoins USDD and FRAX resulting from the cryptocurrency bank default, especially evident in the case of neural networks and random forests. In additional robustness checks, we unveil that (i) BTC is the primary recipient of spillover effects from SIVB, followed by USDC, USDD, and FRAX (in that order) according to a hierarchical tree analysis, and (ii) SIVB primarily impacts Bitcoin, with USDC appearing on a lower branch, in a subsequent Pythagorean forest analysis. Additionally, we conducted a 200-day event study around the date of SVB's bankruptcy, combining price levels and trading volumes, which identifies USDC as a significant channel for financial contagion. These latter findings indicate that advanced modeling techniques, particularly gradient boosting, demonstrate a strong capability in capturing the dynamics of USDC, as well as other stablecoins such as USDT and FRAX.

The remainder of this paper is structured as follows. Sections 2 and 3 contain the descriptions of data and models, respectively. Section 4 outlines the machine learning analysis. Section 5 contains sensitivity analyses. Section 6 concludes the paper.

2. Data

The database covers the time frame from 1 October 2022 to 30 November 2023, with a daily frequency, corresponding to 426 observations. The data are procured from Yahoo Finance and encompass eight variables:

1. *USDC* is Circle's stablecoin USD Coin USD (USDC-USD) in USD.
2. *SIVBQ* is the ticker of the stock price of SIVB Financial Group (SIVBQ) in USD.
3. *BUSD* is Binance's stablecoin BUSD USD (BUSD-USD) in USD.
4. *USDD* is Tron's stablecoin USDD USD (USDD-USD) in USD.
5. *USDT* is Tether's stablecoin USDT USD (USDT-USD) in USD.
6. *FRAX* is Frax Finance's stablecoin USD (FRAX-USD) in USD.
7. *DAI* is MakerDAO Foundation's DAI USD (DAI-USD) in USD.
8. *BTC* is the Bitcoin price (BTC-USD) in USD.

The descriptive statistics for the raw data are provided in Table 2. We note that the minimum values of the stablecoins, which are USDC, FRAX, and DAI, respectively, equal to USD 0.87, USD 0.88, and USD 0.89, are less than USD 1 of their value when they have their peg on the US dollar. BTC and USDT keep their pegs (BTC is even higher than USD 1).

Table 2. Descriptive statistics for raw data from October 2022 to November 2023.

Variable	Mean	Median	Minimum	Maximum
USDC	0.9991	0.9996	0.8774	1.0000
SIVBQ	100.9900	0.5074	0.0100	361.3900
BUSD	0.9994	0.9994	0.9920	1.0014
USDD	0.9914	0.9952	0.9254	0.9994
USDT	0.9997	0.9998	0.9815	1.0059
FRAX	0.9934	0.9951	0.8853	1.0001
DAI	0.9979	0.9985	0.8970	0.9996
BTC	25,140	26,198	15,599	37,617
Variable	St. Error	C.V.	Skewness	Ex. kurtosis
USDC	0.0064	0.0064	-16.9230	302.2600
SIVBQ	125.3500	1.2412	0.5994	-1.3757
BUSD	0.0006	0.0006	-4.9217	43.9130
USDD	0.0084	0.0085	-2.1274	8.5206
USDT	0.0010	0.0010	-10.9020	189.1200
FRAX	0.0080	0.0080	-7.2053	81.8750
DAI	0.0055	0.0055	-15.6570	266.5800
BTC	5444	0.2165	0.0336	-0.5608

Table 2. *Cont.*

Variable	PC 5%	PC 95%	IQ	Obs. missing
USDC	0.9990	0.9999	0.0002	0
SIVBQ	0.0100	315.7300	225.9200	0
BUSD	0.9985	1.0000	0.0004	0
USDD	0.9737	0.9987	0.0094	0
USDT	0.9986	1.0002	0.0004	0
FRAX	0.9849	0.9993	0.0053	0
DAI	0.9960	0.9992	0.0010	0
BTC	16,504	35,301	8225	0

Note: *St. Error* stands for the standard error, *C.V.* for the coefficient of variation, *Ex. kurtosis* for the excess kurtosis, *PC 5%* and *PC 95%* for the 5th and 95th percentiles, respectively, of the data distribution, *IQ* for the interquartile range, and *Obs. missing* for the number of missing observations. Source: Yahoo Finance.

In the analysis provided, the primary variable of interest pertains to the collapse of Silicon Valley Bank’s stock price, denoted as the “input” or triggering event. The main “output” variables under consideration are stablecoins and Bitcoin. Subsequent to the announcement of SIVB’s bankruptcy, investors promptly divested their USDC tokens, leading to the depegging of USDC from the US dollar. This, in turn, precipitated a contagion effect that could have implications for the peg of other stablecoins such as DAI, FRAX, and BUSD. Notwithstanding, ETH and BTC exhibited a degree of resilience to the shock, serving as a haven for investors seeking to offload their USDC tokens regardless of the cost.

For log data, descriptive statistics and plots are given in Table A1 and Figure A1 of Appendix A. In the next section, we detail the machine learning models used.

3. Models

This section outlines the various machine-learning categories that underpin our analysis of the impact of the SIVB collapse on stablecoins.

3.1. Neural Networks

In this section, we elaborate on fully connected neural networks, which are constructed recursively and can encompass an arbitrary number of hidden layers. As we introduce additional hidden layers, the neural network’s capacity expands. Models with three or more hidden layers are commonly referred to as “deep neural” networks.

To create an L -hidden-layer neural network unit, or L -layer unit for brevity, we iteratively apply the process $L - 1$ times. The resulting L -layer unit takes as input a quantity U_{L-1} of $(L - 1)$ -layer units, as follows:

$$f^{(L)}(\mathbf{x}) = a \left(w_0^{(L)} + \sum_{i=1}^{U_{L-1}} w_i^{(L)} f_i^{(L-1)}(\mathbf{x}) \right)$$

We can create a model with $B = U_L$ units in total, where L represents the number of layers in the model.

$$\text{model}(\mathbf{x}, \Theta) = w_0 + f_1^{(L)}(\mathbf{x})w_1 + \dots + f_{U_L}^{(L)}(\mathbf{x})w_{U_L}$$

where

$$f_j^{(L)}(\mathbf{x}) = a \left(w_{0,j}^{(L)} + \sum_{i=1}^{U_{L-1}} w_{i,j}^{(L)} f_i^{(L-1)}(\mathbf{x}) \right) \quad j = 1, 2, \dots, U_L$$

and where the parameter set Θ contains both those weights internal to the neural network units as well as the final linear combination weights. The activation function $a(\cdot)$ commonly includes choices such as the logistic function and the rectified linear unit (ReLU).

$$\text{Logistic: } h(z) = \frac{1}{1 + e^{-z}}, \quad \text{ReLU: } h(z) = \max(0, z).$$

The logistic (or sigmoid) function is commonly employed in the context of logistic regression. It exhibits linear behavior around $z = 0$ and converges to values near 0 and 1 as z decreases or increases. In contrast, the ReLU function is more straightforward, taking the value of z for positive inputs and zero for negative inputs. While the logistic function was historically the standard choice of activation function in neural networks, ReLU has since emerged as the predominant selection in most neural network models, owing to its simplicity and efficacy. Although it is theoretically feasible to utilize different activation functions across various hidden layers within an L -layer unit, for the sake of simplicity, a uniform activation function is almost invariably employed.

3.2. Regression Trees

In this section, we examine the application of general tree-based universal approximators for regression, commonly referred to as regression trees. Tree-based models are often favored for their interpretability relative to neural networks. However, this interpretability diminishes as the depth of the tree increases, particularly when trees are combined or used in an ensemble.

To determine the optimal leaf values for a stump with a fixed split point, we can apply first-order optimality conditions. In the context of regression, the fixed split point s is defined along the n th input dimension of a regression dataset denoted by $\{(x_p, y_p)\}_{p=1}^P$, dividing the data into two sections. These two subsets of the data can be tracked using index sets Ω_L and Ω_R , representing the input/output pairs of the dataset lying on either side of the split, formally expressed as follows:

$$\Omega_L = \{p \mid x_{p,n} \leq s\} \quad \text{and} \quad \Omega_R = \{p \mid x_{p,n} > s\}.$$

The general stump using this split point can be expressed as follows:

$$f(\mathbf{x}) = \begin{cases} v_L & x_n \leq s \\ v_R & x_n > s \end{cases}$$

Here, x_n represents the n th dimension of the input x , while v_L and v_R denote the values of the left and right leaves, respectively. To determine the optimal values for v_L and v_R , we seek to minimize two one-dimensional least squares costs over the points in the index sets Ω_L and Ω_R , as follows:

$$g(v_L) = \frac{1}{|\Omega_L|} \sum_{p \in \Omega_L} (v_L - y_p)^2 \quad \text{and} \quad g(v_R) = \frac{1}{|\Omega_R|} \sum_{p \in \Omega_R} (v_R - y_p)^2$$

where $|\Omega_L|$ and $|\Omega_R|$ represent the cardinality of the index sets Ω_L and Ω_R , respectively. Each of these cost functions is straightforward. By setting the derivative of each to zero with respect to its corresponding leaf value and solving, we obtain the optimal leaf values v_L^* and v_R^* , respectively.

$$v_L^* = \frac{1}{|\Omega_L|} \sum_{p \in \Omega_L} y_p \quad \text{and} \quad v_R^* = \frac{1}{|\Omega_R|} \sum_{p \in \Omega_R} y_p$$

3.3. Boosting with Regression Trees

Boosting involves the learning of a series of weak classifiers, where each classifier aims to rectify the errors made by its predecessors. This method shares similarities with bagging as both are ensemble techniques that amalgamate the predictions of multiple models. Both bagging and boosting can be seen as meta-algorithms, i.e., algorithms constructed on top of other algorithms. Bagging is an ensemble method used to decrease the variance in high-variance base models while boosting is another ensemble method primarily employed to reduce bias in high-bias base models. Boosting operates on the premise that even a weak

high-bias model can often capture some of the relationships between the inputs and the output. By training multiple weak models, each representing a portion of the input-output relationship, it may be possible to integrate the predictions of these models into an overall improved prediction. The objective is to reduce bias by refining an ensemble of weak models into a single robust model.

At the m th round of boosting, we initiate with a model comprising a fully tuned linear combination of $m - 1$ units of a universal approximator. In the case of tree-based units, the bias and weights of the linear combination are already embedded. We express our model as follows:

$$\text{model}_{m-1}(\mathbf{x}, \Theta_{m-1}) = f_{s_1}^*(\mathbf{x}) + f_{s_2}^*(\mathbf{x}) + \cdots + f_{s_{m-1}}^*(\mathbf{x})$$

In the context of the boosted model, each function in this sum represents a tree-based unit, such as a stump, which has been optimized with carefully chosen split points and leaf values. During the m th round of boosting, an extensive search is conducted across a range of suitable candidates, encompassing various trees with differing split points. Subsequently, each candidate's leaf values are meticulously optimized. The construction of the next candidate model involves adding a prospective unit $f_{s_m}(\mathbf{x})$ to $\text{model}_{m-1}(\mathbf{x}, \Theta_{m-1})$, thereby forming the following:

$$\text{model}_m(\mathbf{x}, \Theta_m) = \text{model}_{m-1}(\mathbf{x}, \Theta_{m-1}) + f_{s_m}(\mathbf{x})$$

In order to optimize the leaf values of $f_{s_m}(\mathbf{x})$, it is essential to employ a suitable cost function, such as the least squares cost for regression or the Softmax cost for classification, in relation to a training dataset.

Regarding the leaf-value optimization, consider a scenario where f_{s_m} represents a stump; we address the regression case using the least squares cost, with a dataset containing P points denoted by $\{(x_p, y_p)\}_{p=1}^P$. The objective is to minimize the following pair of least squares costs:

$$g(v_L) = \frac{1}{|\Omega_L|} \sum_{p \in \Omega_L} (\text{model}_{m-1}(\mathbf{x}_p, \Theta_{m-1}) + v_L - y_p)^2$$

$$g(v_R) = \frac{1}{|\Omega_R|} \sum_{p \in \Omega_R} (\text{model}_{m-1}(\mathbf{x}_p, \Theta_{m-1}) + v_R - y_p)^2$$

In order to accurately determine our two leaf values v_L and v_R , where Ω_L and Ω_R represent index sets and $|\Omega_L|$ and $|\Omega_R|$ denote their sizes, we follow a similar approach to cost functions. These simple costs can each be minimized perfectly by verifying the first-order condition for optimality.

Similarly, in the context of two-class classification employing a Softmax cost and label values $y_p \in \{-1, +1\}$, the leaf values of a stump are established by minimizing two costs of the following form:

$$g(v_L) = \frac{1}{|\Omega_L|} \sum_{p \in \Omega_L} \log(1 + e^{-y_p(\text{model}_{m-1}(\mathbf{x}_p, \Theta_{m-1}) + v_L)})$$

$$g(v_R) = \frac{1}{|\Omega_R|} \sum_{p \in \Omega_R} \log(1 + e^{-y_p(\text{model}_{m-1}(\mathbf{x}_p, \Theta_{m-1}) + v_R)})$$

The function in both cases cannot be minimized using a closed-form solution and instead requires local optimization for resolution. This is commonly accomplished by taking a single step using Newton's method, as it offers a favorable balance between accurately minimizing the function and requiring reasonable computational effort.

3.3.1. Gradient Boosting

In this section, we elucidate the application of boosting with regression stumps, a process often construed as successive rounds of fitting to the residual of a regression dataset. This phenomenon is evident even in the case of a simple stump, as demonstrated by the rearrangement of terms. For instance, the expression $g(v_L)$ can be rephrased as follows:

$$g(v_L) = \frac{1}{|\Omega_L|} \sum_{p \in \Omega_L} (v_L - r_p)^2$$

Here, r_p denotes the residual of the p -th data point, defined as $r_p = y_p - \text{model}_{n-1}(\mathbf{x}_p, \Theta_{m-1})$.

3.3.2. Random Forests

A single recursive classification tree is seldom utilized; instead, several trees are aggregated into an ensemble. This process, known as bagging, entails combining multiple cross-validated models to create a single, high-performing model. An alternative approach involves training each tree on a random subset of the original training data and growing them to a predetermined maximum depth before combining them. This method effectively mitigates the overfitting tendencies of individual trees, resulting in highly effective models. In practical terms, training a large number of fully grown tree-based learners often offers advantages over employing a small number of cross-validated ones.

This ensemble of recursively defined trees is commonly referred to as a random forest. The term “random” reflects the practice of using a random subset of the original data to train each tree. Additionally, only a random subset of input feature dimensions is typically sampled to identify viable split points at each node in the trees produced. Within such a forest, approximately $[\sqrt{N}]$ of N features are randomly selected to determine split points in each tree.

3.3.3. Ada Boosting

Adaptive Boosting (AdaBoost) is another popular algorithm for binary classification. Boosting classically attempts to construct a sequence of B (weak) binary classifiers $\hat{y}^{(1)}(\mathbf{x}), \hat{y}^{(2)}(\mathbf{x}), \dots, \hat{y}^{(B)}(\mathbf{x})$. In this procedure, we only consider the final “hard” prediction $\hat{y}(\mathbf{x})$ from the base models and not their predicted class probabilities $g(\mathbf{x})$. Any classification model can, in principle, be used as a base classifier—shallow classification trees are common in practice. The individual predictions of the B ensemble members are then combined into a final prediction. Unlike bagging, all ensemble members are not treated equally. Instead, we assign some positive coefficients $\{\alpha^{(b)}\}_{b=1}^B$ and construct the boosted classifier using a weighted majority vote:

$$\hat{y}_{\text{boost}}^{(B)}(\mathbf{x}) = \text{sign} \left\{ \sum_{b=1}^B \alpha^{(b)} \hat{y}^{(b)}(\mathbf{x}) \right\}.$$

Two critical design considerations for AdaBoost are the selection of the base classifier and the determination of the number of iterations, denoted as B , to execute the boosting algorithm. It is common practice to employ trees of depth one, characterized by two terminal nodes ($M = 2$), as the base classifier. In contrast, the utilization of deep classification trees is generally discouraged due to their potential to compromise performance. The escalation of iterations B can lead to overfitting as an excessive number of base models are utilized, distinguishing AdaBoost from bagging in this regard. It is advisable to methodically select B , for instance, by incorporating early stopping during the training process. AdaBoost demonstrates proficient performance in scenarios characterized by minimal data noise. However, in instances where there is substantial uncertainty in the genuine input-output relationship, the method’s efficacy may diminish. This phenomenon is attributed to the utilization of an exponential loss function in AdaBoost’s formulation, which places significant

penalties on substantial negative margins, rendering it sensitive to noise. Opting for more resilient loss functions can enhance robustness but necessitates a more computationally intensive training regimen.

4. Results

The results are presented in a sequential manner in both the raw and log data formats.

4.1. Raw Data

Over the course of our numerical experiments, we utilized the “input” variable to represent the declining stock price of Silicon Valley Bank, and the “outputs” to denote stablecoins and Bitcoin. Each algorithm yielded a solution after an approximate three-minute computing process.

Drawing from the structural framework presented in Section 3, we endeavored to derive multiple estimates, with some model trials proving unsuccessful. To conserve space, we have opted to organize the results of the models in the paper as follows:

- Neural network (NN);
- Gradient boosting machine (GBM);
- Random forest (RF); and
- Generalized linear model (GLM) as the benchmark.

For each model, a comprehensive set of metrics is provided, including MSE, RMSE, log loss, mean per-class error, and, where available, R-squared. Each model also comes with unique specifications. For instance, NNs report neuron layers, GBM and RF report the number of trees, and GLMs provide elastic net statistics. To streamline the presentation, the confusion matrices have been stored but not printed.

After training a total of three models (in addition to the benchmark), the results of the machine learning testing indicate that GBM is the preferred model, followed by stacked models (including RF), while GLM ranks last. This is evident when examining the MSE and RMSE statistics in Table 3, where GBM minimizes these values. Additionally, the mean per-class error—which is the average of the errors of each class in our dataset—is lower for GBM. For GLM, we also report the null and residual deviances, which provide insights into the predictability of the general linear model for the targeted variable SIVBQ.

Table 3. Machine learning: results with raw data.

	NN	GBM	RF	GLM
MSE	0.8501	0.0640	0.7424	0.6482
RMSE	0.9220	0.2531	0.8616	0.8051
Log loss	3.5095	2.1928	3.6867	2.0509
Mean Per-Class Error	0.8977	0.0586	0.8647	0.6729
R-squared	-	0.9998	0.9997	0.9998
Null Deviance	-	-	-	4110.15
Residual Deviance	-	-	-	1747.45

Regarding the neural network (NN), when predicting SIVBQ, we trained a four-layer neural network with Softmax activation using 4260 training samples. The backpropagation algorithm achieved a dropout rate of 0%. For GBM, the forest size consists of 50 trees, with a mean number of leaves equal to 23 and a mean depth of 5. For RF, the forest size is smaller, with a mean number of leaves equal to 5 and a mean depth of 3.25. For GLM, we also report the following multinomial elastic net statistics: $\alpha = 0.5$ indicates the relative weight of the penalty, while $\lambda = 0.001$ indicates the strength of the regularization.

We ranked variables based on their relative importance, scaled importance, and percentage. Some of the results aligned with our predictions, while others were unexpected. In Table 4, we observe that for the NN, the most influential variable in the model is USDT. Tables 5 and 6 indicate that Bitcoin has the highest impact variable. Finally, in Table 7,

we found that the USDD variable provides better predictions. Overall, Circle's stablecoin USDC ranks 5th and 7th in terms of importance in our experimental designs.

Table 4. Neural network: variable importance ranking for raw data.

NN		Variable Importances Relative Importance	Scaled Importance	Percentage
1	USDT	1.0000	1.0000	0.1578
2	BTC	0.9386	0.9386	0.1481
3	USDD	0.9342	0.9342	0.1474
4	BUSD	0.9178	0.9178	0.1449
5	USDC	0.8839	0.8839	0.1395
6	FRAX	0.8704	0.8704	0.1374
7	DAI	0.7894	0.7894	0.1246

Table 5. Gradient boosting machine: variable importance ranking for raw data.

GBM		Variable Importances Relative Importance	Scaled Importance	Percentage
1	BTC	761.9681	1.0000	0.5010
2	USDD	488.0863	0.6405	0.3209
3	FRAX	147.0443	0.1929	0.0966
4	USDT	39.7943	0.0522	0.0261
5	USDC	36.8304	0.0483	0.0242
6	BUSD	32.9610	0.0432	0.0216
7	DAI	13.9559	0.0183	0.0091

Table 6. Random forest: variable importance ranking for raw data.

RF		Variable Importances Relative Importance	Scaled Importance	Percentage
1	BTC	3517.4062	0.5945	0.2572
2	BUSD	2091.3347	0.5858	0.1529
3	USDD	2060.6845	0.5579	0.1506
4	FRAX	1962.4714	0.4816	0.1435
5	USDT	1694.1772	0.3703	0.1238
6	DAI	1302.8190	0.0432	0.0952
7	USDC	1045.3087	0.2971	0.0764

Table 7. Generalized linear model: variable importance ranking for raw data.

GLM		Variable Importances Relative Importance	Scaled Importance	Percentage
1	USDD	421.5063	1.0000	0.2288
2	BTC	403.1773	0.9565	0.2188
3	FRAX	332.3864	0.7885	0.1804
4	USDT	276.5817	0.6561	0.1501
5	BUSD	266.7639	0.6328	0.1448
6	DAI	123.5459	0.2931	0.0670
7	USDC	18.0070	0.0427	0.0097

In Figure 3, we present the training classification errors for each model. We observed that for the NN, the number of completed passes through the training data is satisfactory after 8 epochs. For GBM and RF, any misclassification seems to be avoided after training a number of trees equal to 10. Lastly, for GLM, the number of iterations to fit the linear model is equal to 5.

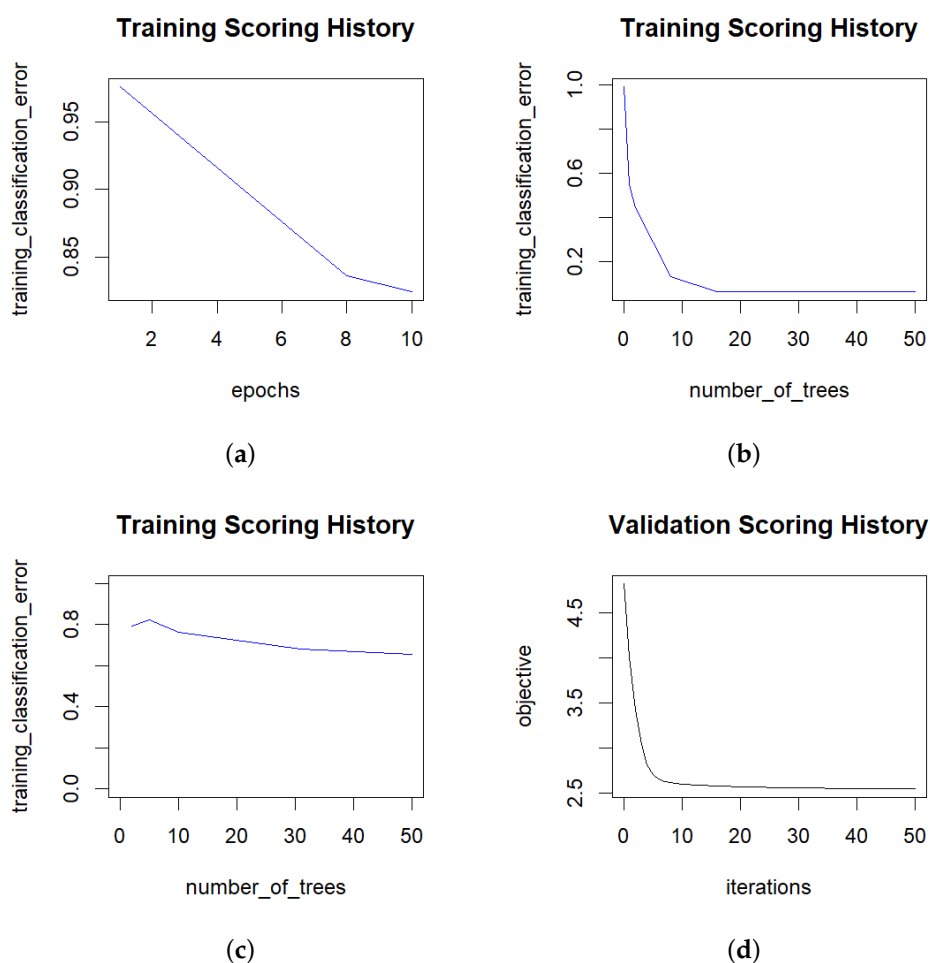


Figure 3. Machine learning training classification errors for raw data. Note: (from left to right and top to bottom): (a) neural network; (b) GBM; (c) random forest; (d) GLM as the benchmark.

4.2. Log Data

Subsequently, we run the models using log data. To review the data, please refer to Table A1 and Figure A1 in Appendix A.

In Tables 8–12, we re-estimate the machine learning models with log data. The overall ranking of competing models remains consistent: GBM continues to emerge as the best-performing model, as evidenced by the analysis of MSE, RMSE, log loss, and mean per-class errors (Table 8).

In the remaining four tables presenting variable importances (Tables 9–12), there are no notable changes in variable ranking for GBM and GLM. As for the primary changes, it is noteworthy that in the case of NN in log form, USDD ranks first with 16.15%, and FRAX ascends to the fourth rank. This suggests that the collapse of SIVB ultimately had an impact on these two stablecoins. Furthermore, for RF in log form, the relative importance of BTC decreases to 21.81%, and BUSD now ranks fifth. Regarding the evolution of BUSD, it is essential to remember that Binance stablecoin was removed from the exchanges shortly after our database ended (see <https://www.binance.com/en/square/post/693476806441> (accessed on 12 April 2024)). FRAX ascends to third place (15.7%) in terms of variable importance, with USDD in second place, which aligns with previous findings for NN.

Table 8. Machine learning: results with log data.

	NN	GBM	RF	GLM
MSE	0.8368	0.0641	0.7692	0.6482
RMSE	0.9147	0.2531	0.8771	0.8052
Log loss	3.4271	2.1929	3.6139	2.051
Mean per-class error	0.9189	0.0557	0.8686	0.6729
R-squared	-	0.9999	0.9998	0.9998
Null deviance	-	-	-	4110.15
Residual deviance	-	-	-	1747.45

Table 9. Neural network: variable importance ranking for log data.

NN		Variable Importances Relative Importance	Scaled Importance	Percentage
1	USDD	1.0000	1.0000	0.1615
2	BTC	0.9985	0.9985	0.1613
3	USDT	0.9361	0.9361	0.1512
4	FRAX	0.8603	0.8603	0.139
5	USDC	0.8188	0.8188	0.1323
6	BUSD	0.8104	0.8104	0.1309
7	DAI	0.7652	0.7652	0.1236

Table 10. Gradient boosting machine: variable importance ranking for log data.

GBM		Variable Importances Relative Importance	Scaled Importance	Percentage
1	BTC	761.9682	1.0000	0.5011
2	USDD	488.0864	0.6406	0.3209
3	FRAX	147.0443	0.193	0.0966
4	USDT	39.7944	0.0522	0.0261
5	USDC	36.8304	0.0483	0.0242
6	BUSD	32.9611	0.0432	0.0217
7	DAI	13.956	0.0183	0.0092

Table 11. Random forest: variable importance ranking for log data.

RF		Variable Importances Relative Importance	Scaled Importance	Percentage
1	BTC	2978.0828	1.0000	0.2181
2	USDD	2182.5	0.7328	0.1599
3	FRAX	2143.5813	0.7198	0.157
4	USDT	2092.3237	0.7026	0.1532
5	BUSD	1772.5676	0.5952	0.1298
6	DAI	1406.6959	0.4723	0.103
7	USDC	1076.8752	0.3616	0.0789

Table 12. Generalized linear model: variable importance ranking for log data.

GLM		Variable Importances Relative Importance	Scaled Importance	Percentage
1	USDD	421.5063	1.0000	0.2288
2	BTC	403.1773	0.9565	0.2188
3	FRAX	332.3864	0.7885	0.1804
4	USDT	276.5817	0.6561	0.1501
5	BUSD	266.7639	0.6328	0.1448
6	DAI	123.5459	0.2931	0.0670
7	USDC	18.0070	0.0427	0.0097

In Figure 4, we account for the classification errors of machine learning training in logarithmic form. The same comments apply.

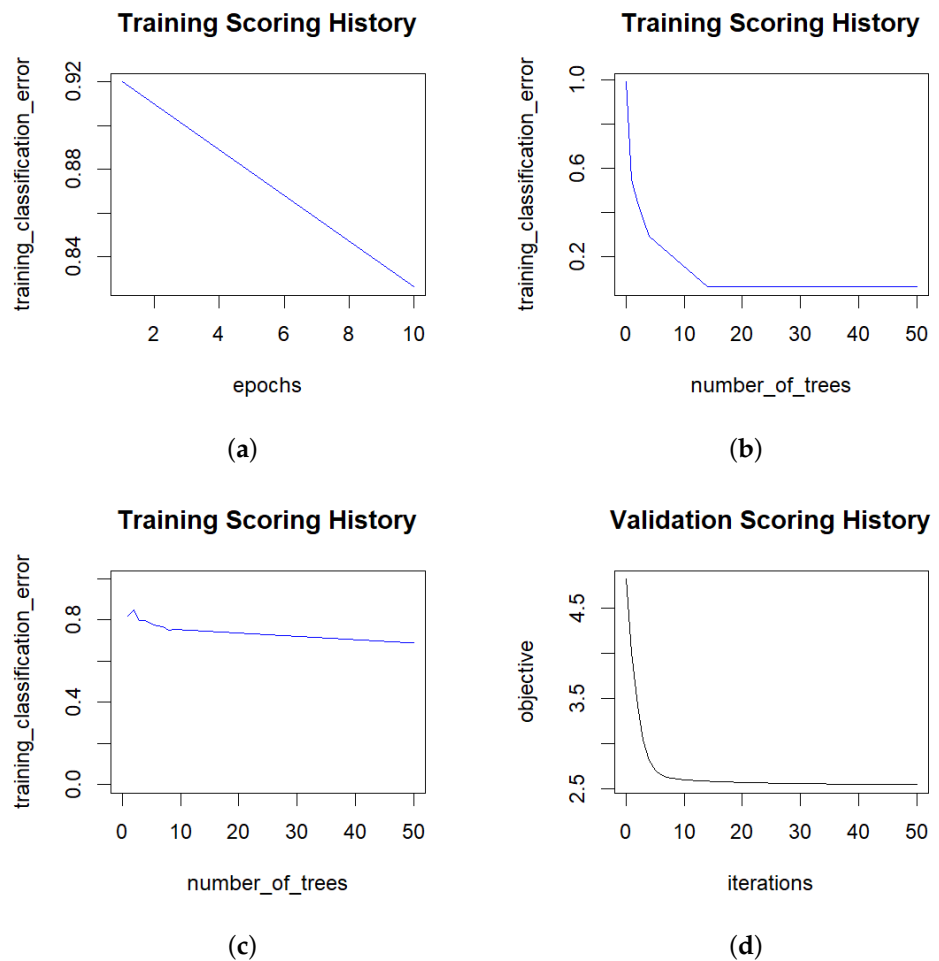


Figure 4. Machine learning training classification errors for log data. Note: (from left to right and top to bottom): (a) neural network; (b) GBM; (c) Random Forest; (d) GLM as the benchmark.

5. Robustness Tests

To gain a deeper understanding of the insights obtained from our database, encompassing the Silicon Valley Bank stock, the USDC depeg, and additional stablecoins (USDT, USDD, FRAX, DAI), we conduct several visualization exercises in this section.

5.1. Hierarchical Tree

First, we consider the hierarchical decision tree, a fundamental algorithm that segments data into nodes based on class purity [21,22]. This algorithm serves as the foundation for the random forest algorithm. Interested readers can click on the image to view a full-size version of the tree.

The decision tree presented in Figure 5 (depicting the full tree) and Figure 6 (providing a zoomed-in view) begins with an analysis of the impact of SIVB’s default on Bitcoin. The tree then diverges into two paths: (i) USDT on the left, and (ii) USDC on the right. Our primary focus lies on the USDC path to investigate the repercussions of SIVBQ on USDC’s depeg. At the third sub-branch, the analysis reveals that USDC exerts spillover effects on USDT, followed by USDD (at the fourth sub-branch), and subsequently FRAX at the fifth sub-branch. Notably, BUSD and DAI stablecoins appear to be minimally impacted by any spillover effects emanating from USDC.

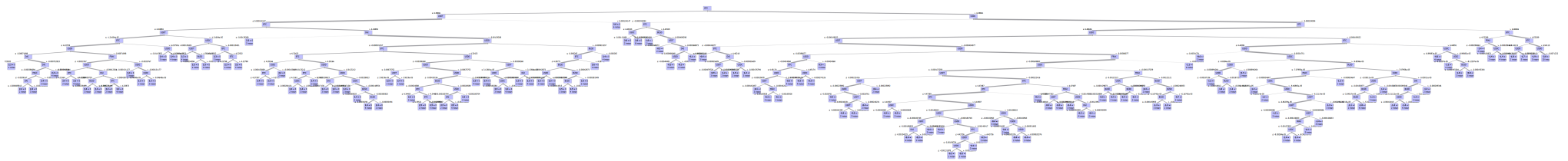


Figure 5. Decision tree learning algorithm for stablecoins using the SIVBQ-trained model. Note: The target is SIVBQ. Figure 6 provides the reader with a zoomed-in picture on the right-hand side.

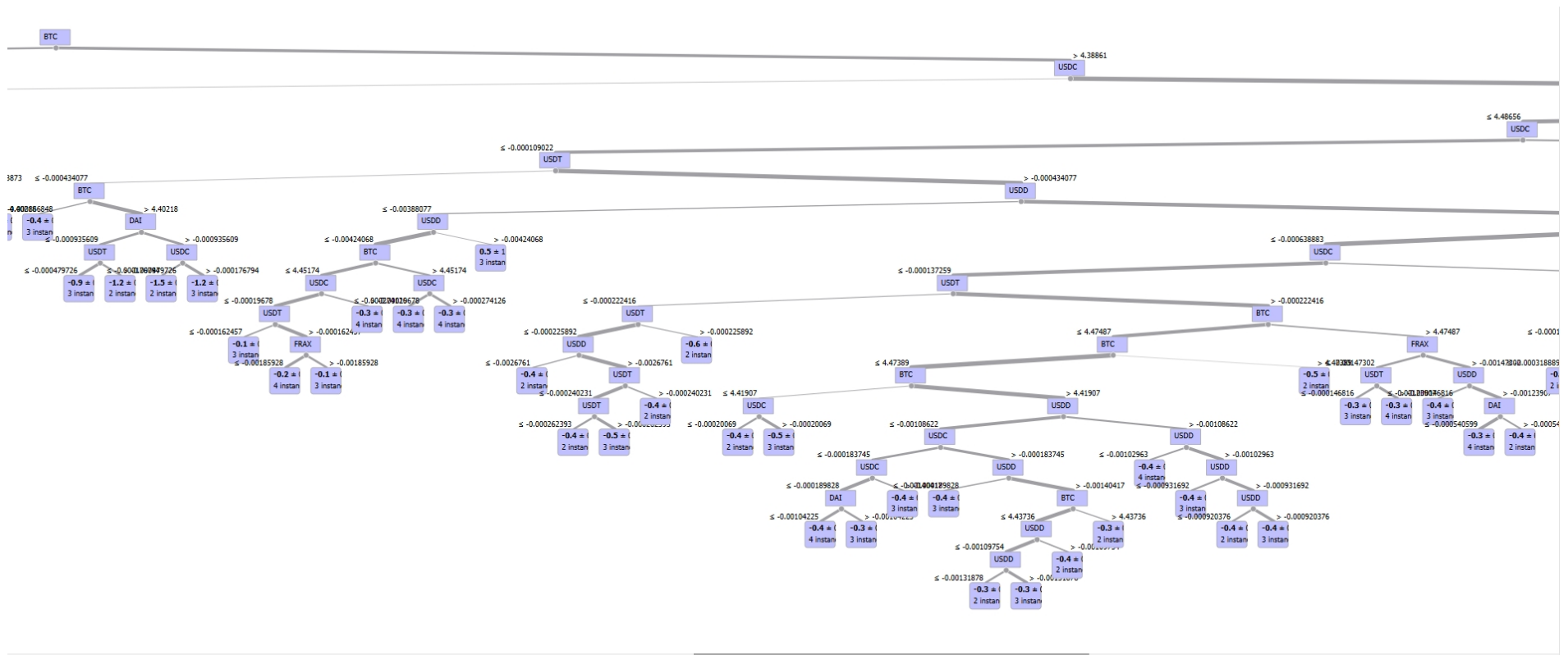


Figure 6. Zoomed-in picture of the decision tree on the right-hand side. Note: The target is SIVBQ. This Figure provides the reader with a zoomed-in picture of the USDC path on the right-hand side of the hierarchical tree.

5.2. Pythagorean Forest

Second, we explore a variant of the decision tree called the Pythagorean forest [23], which aims to mitigate the tendency of the classification tree to overfit the data.

The Pythagorean forest encompasses all the decision tree models derived from the Random Forest trained for SIVBQ. Within Figure 7, these trees are depicted as Pythagorean trees, with each visualization corresponding to a randomly generated tree.

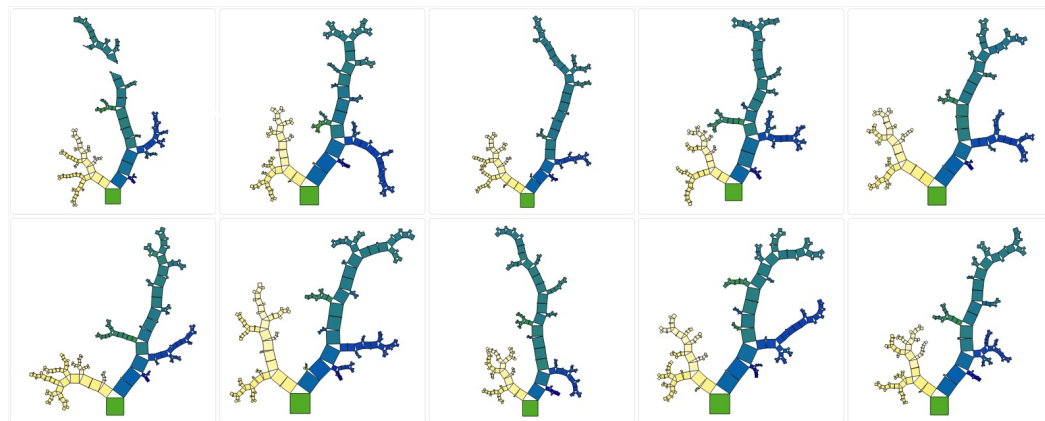


Figure 7. Pythagorean forest among stablecoins. Note: The target is SIVBQ. The color palette corresponds to a split in “mean” values.

The tree with the shortest and most vividly colored branches is considered the optimal tree. After considering various options, our focus narrowed down to trees number three and ten.

In terms of the relationship between parent and child nodes, it is assumed that SIVBQ predominantly assigns Bitcoin to the left split of the tree, while the remaining stablecoins are allocated to the right split. Notably, USDD is represented in blue and USDC in green. Upon visual observation, it is evident that the spillover effects of SIVB default on USDC are considerably greater than those on USDD.

Overall, these additional plots have provided a wealth of insights into the impact of Silicon Valley Bank’s decline on the stablecoin markets.

5.3. Event Study with Volumes Analysis

As a concluding sensitivity analysis, we implement an “event study” approach by re-estimating Tables 3–7 over a defined window. This window begins 100 days prior to the SVB collapse, starting on 1 December 2022, and extending to 100 days following the event, concluding on 19 June 2023. The triggering event for this analysis is the SVB collapse that occurred on 11 March 2023.

Table 13 presents a comprehensive summary of the performance metrics for the various machine learning models utilized in this analysis. The gradient boosting machine (GBM) demonstrated the highest level of effectiveness in evaluating the impact of the SVB bankruptcy throughout this event study, achieving the lowest values for the mean squared error (MSE), root mean squared error (RMSE), and mean absolute error (MAE). These results highlight its robust capability in analyzing non-linear relationships.

Additionally, this latter model, combining both price levels and traded volumes data, yielded an impressive R-squared value of 0.9933, indicating its superior ability to account for variability within the data and significantly surpassing the performance of alternative models, such as random forest and neural networks. Conversely, the generalized linear model (GLM) recorded the lowest R-squared value of 0.5681, illustrating the difficulties encountered in capturing the intricate dynamics at work. This emphasizes the importance of employing more sophisticated models to effectively analyze financial contagion.

Table 13. Event study: performance metrics for machine learning models.

Model	MSE	RMSE	MAE	Mean Residual Deviance	R-Squared
Neural Network	3714.656	60.94798	51.19611	3714.656	0.7595
Gradient Boosting	104.1134	10.2036	6.466536	104.1134	0.9933
Random Forest	858.7121	29.30379	19.40733	858.7121	0.9444
Generalized Linear	6671.447	81.67893	70.31123	6671.447	0.5681

Note: The event study analyzed a 200-day period from 1 December 2022 to 19 June 2023. A significant milestone that differentiates the sample into two equal segments is the bankruptcy of SVB, which took place on 11 March 2023. The statistics presented in this table encompass both price levels and trading volumes.

In Table 14, the neural network analysis highlights Bitcoin (BTC) as the most significant variable, comprising 30.66% of the importance. This emphasizes its function as a safe-haven asset during times of financial uncertainty. Following Bitcoin, USDC ranks second with a share of 16.07%, indicating its sensitivity to the collapse of Silicon Valley Bank (SVB), primarily due to its reliance on traditional banking reserves. Additionally, other stablecoins, such as USDT at 13.35% and FRAX at 12.34%, demonstrate moderate importance, suggesting they are partially affected by the spillover effects originating from USDC.

Table 14. Variable importance for the neural network (NN).

Variable	Relative Importance	Scaled Importance	Percentage
BTC	1.0000	1.0000	0.3066
USDC	0.5241	0.5241	0.1607
USDT	0.4354	0.4354	0.1335
FRAX	0.4023	0.4023	0.1234
BUSD	0.3702	0.3702	0.1135
DAI	0.2957	0.2957	0.0907
USDD	0.2336	0.2336	0.0716

In Table 15, Bitcoin demonstrates a dominant position in the random forest analysis with a significant contribution of 55.13%, underscoring its resilience during periods of financial instability. Following Bitcoin, USDT and USDD account for 16.02% and 10.17%, respectively, highlighting their relative significance within the contagion framework. Notably, USDC ranks lowest at 2.45%, which may suggest that the random forest analysis prioritizes broader market dynamics over specific reserve impacts.

Table 15. Variable importance for random forest (RF).

Variable	Relative Importance	Scaled Importance	Percentage
BTC	67,023,708	1.0000	0.5513
USDT	19,474,388	0.2906	0.1602
USDD	12,368,518	0.1845	0.1017
FRAX	9,449,935	0.1410	0.0777
DAI	6,082,494.5	0.0907	0.05
BUSD	4,191,192.75	0.0625	0.0345
USDC	2,976,298.25	0.0444	0.0245

In Table 16, the gradient boosting model (GBM) emphasizes the dominant role of Bitcoin, which accounts for 92.34% of the overall importance, underscoring its significance in the market. In comparison, USDC is positioned as a secondary variable at 2.12%, reflecting its inherent vulnerabilities despite a lower level of relative importance. Additionally, stablecoins such as DAI (2%) and BUSD (1.51%) exhibit minimal influence, consistent with their nature as safer, asset-backed alternatives.

Table 16. Variable importance for gradient boosting machines (GBMs).

Variable	Relative Importance	Scaled Importance	Percentage
BTC	14,989,162	1.0000	0.9234
USDC	344,378.90625	0.0230	0.0212
DAI	324,389.25	0.0216	0.0200
BUSD	245,349.6875	0.0164	0.0151
USDT	141,211.71875	0.0094	0.0087
FRAX	94,800.9140625	0.0063	0.0060
USDD	93,014.15625	0.0062	0.0057

In Table 17, the analysis of the generalized linear modeling (GLM) underscores the prominence of Bitcoin, which constitutes 47.32% of the total importance, thereby affirming its resilience in times of crisis. Notably, the analysis attributes greater significance to DAI (16.57%) and FRAX (13.78%) in comparison to USDC (6.49%). This finding prompts a careful examination of potential biases inherent in the linear modeling methodology, particularly concerning the assessment of non-major stablecoins.

Table 17. Variable importance for generalized linear modeling (GLM).

Variable	Relative Importance	Scaled Importance	Percentage
BTC	80.0206	1.0000	0.4732
DAI	28.0221	0.3502	0.1657
FRAX	23.3003	0.2912	0.1378
USDT	22.1145	0.2764	0.1308
USDC	10.9733	0.1371	0.0649
USDD	3.2839	0.0410	0.0194
BUSD	1.3977	0.0175	0.0083

In conclusion, the findings from the machine learning models indicate that Bitcoin functions consistently as a stabilizing force within the cryptocurrency market during systemic shocks, such as the recent collapse of Silicon Valley Bank (SVB). The significance of USDC is critical yet varies across the models, demonstrating its dual role as both a systemic vulnerability and a channel for contagion. Furthermore, advanced modeling methodologies, such as geometric Brownian motion (GBM), have shown superior performance compared to traditional methods in capturing these complex dynamics. This underscores the necessity for more sophisticated analytical tools to assess financial contagion and the resilience of stablecoins effectively.

6. Conclusions

The stablecoin market experienced a notable impact when USD Coin deviated from its peg to the US dollar [24] on 11 March 2023. This deviation occurred as a result of a sell-off following the bankruptcy of Silicon Valley Bank, where Circle had deposited funds to ensure the stability of its peg. As USDC plays a critical role in the collateral system, other major stablecoins also began to lose their peg to the US dollar [25]. The depegging of USD Coin and the subsequent contagion effect within the DeFi ecosystem illustrate the profound interconnectedness and systemic risks within the cryptocurrency market. Further, the collapse of Silicon Valley Bank revealed vulnerabilities in centralized institutions, triggering a domino effect across various stablecoins and cryptocurrencies, as well as in the banking environment. Indeed, the collapse of SIVB significantly destabilized and endangered the banking sector, as evidenced by the takeovers of Credit Suisse and First Republic Bank [26].

In this paper, we present the findings of a series of machine learning experiments, encompassing nonlinear regression, neural network analysis, gradient boosting machines, and random forests. These experiments aimed to investigate the repercussions of SIVB's collapse on the stablecoins USDC, USDD, BUSD, DAI, and FRAX, in conjunction with USDT and BTC as global benchmarks. The study utilized daily data spanning from October 2022 to November 2023. The key findings are as follows:

1. The gradient boosting machine (GBM) exhibited superior performance in terms of loss scores compared to other machine learning models.
2. Notably, the impact of SIVB's collapse on stablecoins USDD and FRAX was revealed, particularly through neural networks and random forests.
3. Sensitivity analyses highlighted that USDC ranked second in importance after Bitcoin in the hierarchical tree, indicating its vulnerability to the SIVB collapse.
4. Circle's stablecoin emerged as the third most important variable according to the Pythagorean forest, underscoring its significance as a primary variable of interest.
5. The event study, which integrates price levels and volume data, demonstrates that USDC functions as both a systemic vulnerability and a potential contagion channel. Furthermore, it emphasizes the varying significance of other stablecoins within this context.

Overall, our analysis highlights the necessity of employing advanced analytical tools to effectively evaluate the resilience of stablecoins during times of crisis. The depegging of USD Coin subsequent to the collapse of Silicon Valley Bank sheds light on the intricate and sometimes precarious relationships between stablecoins and traditional financial institutions. USDC, which is designed to maintain a 1:1 peg with the US dollar, experienced significant volatility when SIVB, a major banking partner, failed. This event led to a temporary loss of confidence among investors, causing USDC to trade below its intended value. The incident underscores several key points. Firstly, the reliance of stablecoins on banking institutions for liquidity and reserves makes them vulnerable to traditional financial sector disruptions. Secondly, the rapid and transparent response from Circle, the issuer of USDC, played a crucial role in restoring stability, emphasizing the importance of robust crisis management and communication strategies in the crypto space. Finally, this episode serves as a reminder of the need for regulatory clarity and stronger financial safeguards to ensure the resilience of digital assets against unforeseen financial shocks. In conclusion, the USDC depegging incident post-SIVB collapse underscores the delicate balance stablecoins must maintain between digital innovation and traditional financial dependencies. It calls for enhanced regulatory oversight and more resilient financial infrastructures to support the growing integration of digital assets into the broader financial ecosystem. In Europe, for instance, the Markets in Crypto-Assets (MiCa) directive aims to protect retail holders from such turmoils in the cryptocurrency markets [27].

The recent occurrence underscores the significance of implementing robust risk management strategies and emphasizes the need for enhanced transparency and regulatory oversight within the DeFi space. As the cryptocurrency market continues to evolve, it is increasingly imperative for market participants to establish resilient frameworks and collaborate toward fostering a more stable and sustainable ecosystem for digital assets.

Author Contributions: Conceptualization, P.O.D. and J.C.; methodology, P.O.D., J.C., and B.S.; software, P.O.D. and B.S.; validation, J.C.; formal analysis, P.O.D.; data curation, P.O.D. and B.S.; writing—original draft preparation, P.O.D. and J.C.; writing—review and editing, P.O.D., J.C., and B.S.; visualization, P.O.D. and B.S.; supervision, J.C. and B.S.; project administration, P.O.D. and J.C. All authors have read and agreed to the published version of the manuscript.

Funding: This research received no external funding.

Institutional Review Board Statement: Not applicable.

Informed Consent Statement: Not applicable.

Data Availability Statement: The stablecoins and SIVB data are freely available from Yahoo Finance! <https://finance.yahoo.com/> (accessed on 12 April 2024).

Conflicts of Interest: The authors declare no conflicts of interest.

Appendix A

Table A1. Descriptive Statistics for Log Data from October 2022 to November 2023.

Variable	Mean	Median	Minimum	Maximum
USDC	−0.0003	−0.0001	−0.0568	0.0001
SIVBQ	0.4874	−0.2946	−2.0000	2.5580
BUSD	−0.0002	−0.0002	−0.0034	0.0005
USDD	−0.0037	−0.0020	−0.0336	−0.0002
USDT	−0.0001	−0.0005	−0.0080	0.0025
FRAX	−0.0028	−0.0020	−0.0529	0.0002
DAI	−0.0009	−0.0006	−0.0472	−0.0001
BTC	4.3897	4.4183	4.1931	4.5754
Variable	St. error	C.V.	Skewness	Ex. kurtosis
USDC	0.0029	7.8797	−17.1070	308.5600
SIVBQ	1.6611	3.4077	0.1057	−1.6846
BUSD	0.0002	1.0919	−4.9432	44.2220
USDD	0.0037	1.0011	−2.2086	9.4024
USDT	0.0004	3.9918	−11.0200	191.4200
FRAX	0.0036	1.2601	−7.6188	90.1630
DAI	0.0025	2.7854	−15.8610	272.8500
BTC	0.0980	0.0223	−0.3862	−0.7230
Variable	PC 5%	PC 95%	IQ	Obs. missing
USDC	−0.0004	−0.0001	0.0001	0
SIVBQ	−2.0000	2.4993	3.3999	0
BUSD	−0.0006	0.0001	0.0002	0
USDD	−0.0115	−0.0005	0.0041	0
USDT	−0.0005	0.0001	0.0001	0
FRAX	−0.0066	−0.0002	0.0023	0
DAI	−0.0017	−0.0003	0.0001	0
BTC	4.2176	4.5478	0.1463	0

Note: *St. Error* stands for the Standard Error, *C.V.* for the Coefficient of Variation, *Ex. kurtosis* for the excess kurtosis, *PC 5%* and *PC 95%* for the 5th and 95th percentile respectively of the data distribution, *IQ* for the Interquartile Range, and *Obs. missing* for the number of missing observations. Source: Yahoo Finance.

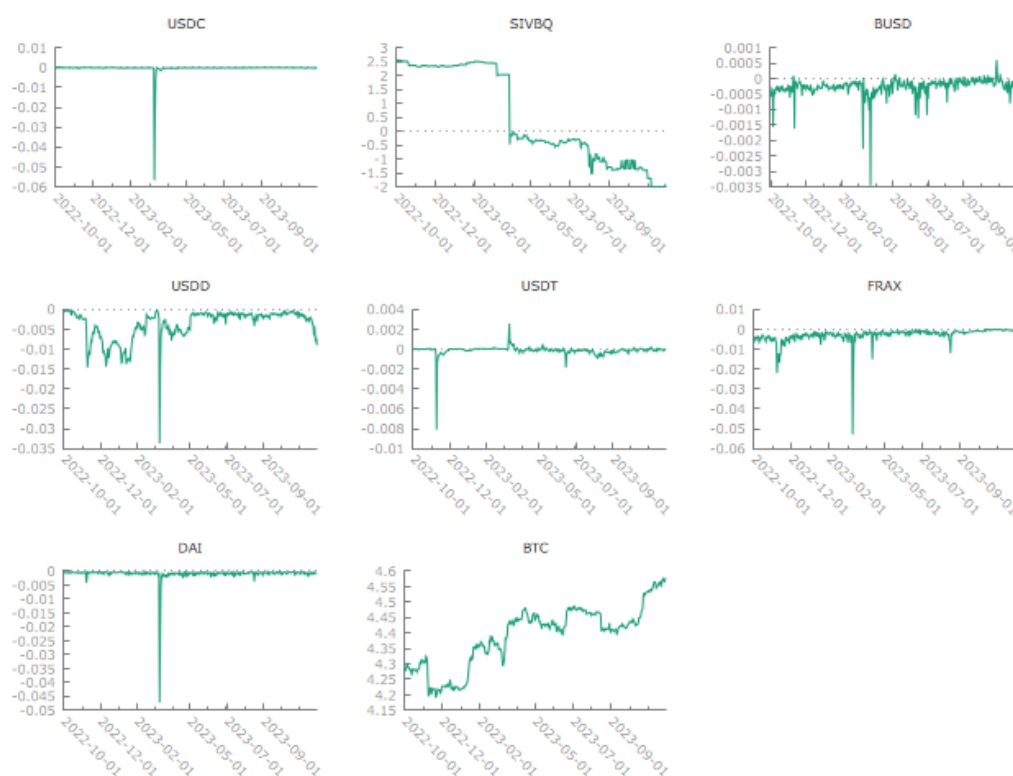


Figure A1. Database in Log Data from October 2022 to November 2023. Note: From top to bottom and left to right, *USDC* is Circle’s stablecoin in USD, *SIVBQ* is the ticker of the stock price for SIVB Financial Group in USD, *BUSD* is Binance’s stablecoin in USD, *USDD* is Tron’s stablecoin in USD, *USDT* is Tether’s stablecoin in USD, *FRAX* is Frax Finance’s stablecoin USD in USD, *DAI* is MakerDAO Foundation’s DAI in, and *BTC* is the Bitcoin price in USD. Source: Yahoo Finance.

References

1. Yousaf, I.; Riaz, Y.; Goodell, J.W. The impact of the SVB collapse on global financial markets: Substantial but narrow. *Financ. Res. Lett.* **2023**, *55*, 103948. [CrossRef]
2. Pandey, D.K.; Hassan, M.K.; Kumari, V.; Hasan, R. Repercussions of the Silicon Valley Bank collapse on global stock markets. *Financ. Res. Lett.* **2023**, *55*, 104013. [CrossRef]
3. Aharon, D.Y.; Ali, S.; Naved, M. Too big to fail: The aftermath of Silicon Valley Bank (SVB) collapse and its impact on financial markets. *Res. Int. Bus. Financ.* **2023**, *66*, 102036. [CrossRef]
4. Time, T.E. Crypto shaken as SVB exposure Depegs \$37 billion Stablecoin. *The Economic Times*, 12 March 2023.
5. Lv, S.; Du, Y.; Liu, Y. How do fintechs impact banks’ profitability?—An empirical study based on banks in China. *FinTech* **2022**, *1*, 155–163. [CrossRef]
6. Cintra, T.N.; Holloway, M.P. Detecting Depegs: Towards Safer Passive Liquidity Provision on Curve Finance. *arXiv* **2023**, arXiv:2306.10612.
7. Anadu, K.; Azar, P.; Huang, C.; Cipriani, M.; Eisenbach, T.M.; La Spada, G.; Landoni, M.; Macchiavelli, M.; Malfroy-Camine, A.; Wang, J.C. *Runs and Flights to Safety: Are Stablecoins the New Money Market Funds?* FRB of Boston Supervisory Research & Analysis Unit: Boston, MA, USA, 2023.
8. Kozhan, R.; Viswanath-Natraj, G. *Decentralized Stablecoins and Collateral Risk*; WBS Finance Group Research Paper; Warwick Business School: Coventry, UK, 2021.
9. Sween, S. Contagion Risks of Stablecoins: Investor-level Evidence from the Terra Shock. SSRN 4473042, 2023. Available online: https://papers.ssrn.com/sol3/papers.cfm?abstract_id=4473042 (accessed on 12 April 2024).
10. Griffin, J.M.; Shams, A. Is Bitcoin really untethered? *J. Financ.* **2020**, *75*, 1913–1964. [CrossRef]
11. Kristoufek, L. Tethered, or Untethered? On the interplay between stablecoins and major cryptoassets. *Financ. Res. Lett.* **2021**, *43*, 101991. [CrossRef]
12. Kwon, Y.; Pongmala, K.; Qin, K.; Klages-Mundt, A.; Jovanovic, P.; Parlour, C.; Gervais, A.; Song, D. What Drives the (In) stability of a Stablecoin? *arXiv* **2023**, arXiv:2307.11754.
13. Grobys, K.; Junttila, J.; Kolari, J.W.; Sapkota, N. On the stability of stablecoins. *J. Empir. Financ.* **2021**, *64*, 207–223. [CrossRef]
14. Lyons, R.K.; Viswanath-Natraj, G. What keeps stablecoins stable? *J. Int. Money Financ.* **2023**, *131*, 102777. [CrossRef]
15. Kristoufek, L. On the role of stablecoins in cryptoasset pricing dynamics. *Financ. Innov.* **2022**, *8*, 37. [CrossRef]

16. White, L.H. Should We Fear Stablecoins? *Policy Commons*, 24 June 2021.
17. Simmons, R. Monetary Transmission & Small Firm Credit Rationing: The Stablecoin Opportunity to Raise Business Credit Flows. *FinTech* **2024**, *3*, 379–406. [CrossRef]
18. Lee, E.; Chiu, Y.F.; Hsieh, M.H. Stablecoin Depegging Risk Prediction. SSRN 4700764, 2024. Available online: https://papers.ssrn.com/sol3/papers.cfm?abstract_id=4700764 (accessed on 12 April 2024).
19. Bullmann, D.; Klemm, J.; Pinna, A. In Search for Stability in Crypto-Assets: Are Stablecoins the Solution? SSRN 3444847, 2019. Available online: https://papers.ssrn.com/sol3/papers.cfm?abstract_id=3444847 (accessed on 12 April 2024).
20. LeDell, E.; Poirier, S. H2o automl: Scalable automatic machine learning. In Proceedings of the AutoML Workshop at ICML, ICML, Online, 17–18 July 2020; Volume 2020.
21. Breiman, L. *Classification and Regression Trees*; Routledge: London, UK, 2017.
22. Quinlan, J.R. Induction of decision trees. *Mach. Learn.* **1986**, *1*, 81–106. [CrossRef]
23. Beck, F.; Burch, M.; Munz, T.; Di Silvestro, L.; Weiskopf, D. Generalized pythagoras trees for visualizing hierarchies. In Proceedings of the 2014 International Conference on Information Visualization Theory and Applications (IVAPP), Lisbon, Portugal, 5–8 January 2014; IEEE: Piscataway, NJ, USA, 2014; pp. 17–28.
24. Erer, E.; Erer, D. The domino effect of silicon valley Bank’s bankruptcy and the role of FED’s monetary policy. *Borsa Istanbul Rev.* **2024**, *24*, 573–591. [CrossRef]
25. Azmi, W.; Anwer, Z.; Azmi, S.N.; Nobanee, H. How did major global asset classes respond to Silicon Valley Bank failure? *Financ. Res. Lett.* **2023**, *56*, 104123. [CrossRef]
26. Akhtaruzzaman, M.; Boubaker, S.; Goodell, J.W. Did the collapse of Silicon Valley Bank catalyze financial contagion? *Financ. Res. Lett.* **2023**, *56*, 104082. [CrossRef]
27. Dragomir, V.D.; Dumitru, V.F. Recognition and Measurement of Crypto-Assets from the Perspective of Retail Holders. *FinTech* **2023**, *2*, 543–559. [CrossRef]

Disclaimer/Publisher’s Note: The statements, opinions and data contained in all publications are solely those of the individual author(s) and contributor(s) and not of MDPI and/or the editor(s). MDPI and/or the editor(s) disclaim responsibility for any injury to people or property resulting from any ideas, methods, instructions or products referred to in the content.